Structure and Interactions of the Single-Stranded DNA Genome of Filamentous Virus *fd*: Investigation by Ultraviolet Resonance Raman Spectroscopy†

Zai Qing Wen, Stacy A. Overman, and George J. Thomas, Jr.*

Division of Cell Biology and Biophysics, School of Biological Sciences, University of Missouri−Kansas City, Kansas City, Missouri 64110

Received February 14, 1997; Revised Manuscript Received April 28, 1997⊗

ABSTRACT: The filamentous bacteriophage *fd* is a member of the *Ff* class of *Inovirus*, which includes phages *f1* and *M13*. Ultraviolet resonance Raman (UVRR) spectra of *fd* have been obtained using excitation wavelengths of 257, 244, 238, and 229 nm. Excitation at 257 nm selectively enhances Raman markers of the packaged single-stranded (ss) DNA genome, while excitation at the shorter wavelengths favors the detection of Raman signals from coat protein aromatics, particularly tryptophan (W26) and tyrosine residues (Y21 and Y24) of the viral coat subunit (pVIII). The principal findings are the following: (1) Distinctive markers of dA, dC, dG, and dT residues of the packaged genome are identified in UVRR spectra of *fd* excited at 257 and 244 nm, despite the low DNA mass composition (12%) of the virion. (2) Raman bands of the bases of packaged ssDNA show extraordinary resonance Raman *hypo*chromism. Raman intensity losses as large as 80% of the parent DNA nucleotide intensities are observed. This is interpreted as evidence of extensive short-range interactions involving bases of the packaged genome. (3) Conversely, Raman bands of tryptophan and tyrosine residues of the coat protein generally exhibit strong *hyper*chromism. Typically, Raman markers of the aromatic amino acids are about 3-fold more intense in the UVRR spectrum of *fd* than in spectra of the free amino acids. The very high Raman cross sections for residues Y21, Y24, and W26 are indicative of unusual hydrophobic environments in the viral assembly. (4) UVRR band shifts that accompany the transfer of *fd* from H_2O to D_2O solution indicate that bases of the packaged ssDNA are readily exchanged by the solvent. Similarly, the indole N1H group of W26 is accessible to solvent, as shown by N1H → N1D exchange in D_2O solution. (5) The UVRR markers of the packaged *fd* genome confirm the conclusion reached previously from off-resonance Raman studies that *fd* DNA nucleosides favor the C3′-*endo/anti* conformation, rather than the C2′-*endo/anti* conformation that is characteristic of the lowest energy structure of DNA. We conclude that nucleoside conformations of the packaged *fd* genome are influenced by the specific organization of ssDNA and coat protein subunits in the native virion assembly.

Bacteriophage *fd* is the prototype of the long and thin *Ff* filamentous viruses (*Inovirus*) which infect F^+ strains of *Escherichia coli*. Included in the *Ff* class are the closely related bacteriophages *f1* and *M13*. Each contains a single-stranded (ss) DNA loop of ∼6400 nucleotides within a protein coat comprising ∼2700 copies of a 50-residue subunit (Day et al., 1988). The use of *Ff* virions as cloning vectors, vehicles for antigen display, and models of nucleoprotein assembly within a membrane bilayer has made the filamentous architecture a frequent target of investigation by spectroscopic and diffraction methods (Cross et al., 1983; Aubrey & Thomas, 1991; Arnold et al., 1992; Clack & Gray, 1992; Glucksman et al., 1992; McDonnell et al., 1993; Marvin et al., 1994; Overman et al., 1994; Overman & Thomas, 1995; Symmons et al., 1995; Takeuchi et al., 1996; Tsuboi et al., 1996). Structural models have been proposed which incorporate the results of X-ray fiber diffraction (Glucksman et al., 1992; Marvin et al., 1994), solid-state NMR spectroscopy (McDonnell et al., 1993), and solution and fiber Raman spectroscopy (Overman et al., 1996; Tsuboi et al., 1996; Takeuchi et al., 1996). These studies have focused primarily on the α-helical secondary structure and relative orientation of the coat protein subunit (pVIII) within the virion assembly. Less well understood is the conformation of the internally packaged ssDNA genome and its structural relationship to the protein coat. Because the packaged ssDNA molecule constitutes only 12% of the virion mass, investigation of its structure has presented a considerable challenge in both spectroscopic and diffraction analyses.

Ultraviolet resonance Raman (UVRR) spectroscopy has the sensitivity required to probe the ssDNA component of the *Ff* assembly, and thus provides a valuable complement to other structural methods. In the UVRR approach, the laser-excitation frequency is tuned into resonance with the target chromophore, and thereby an intense Raman spectrum of the chromophore is selectively obtained. Reviews of applications of UVRR spectroscopy to nucleic acids and proteins have been given (Tsuboi et al., 1987; Thomas & Tsuboi, 1993; Austin et al., 1993). Although the UVRR method has been effective in investigating nucleic acids and proteins separately, few applications to nucleoprotein assemblies, such as viruses, have been reported (Grygon et al., 1988; Tuma et al., 1996). The feasibility of UVRR spectroscopy for virus studies has recently been advanced by improvements in laser sources and detectors (Asher et al., 1993; Russell et al., 1995).

† Paper LVI in the series Structural Studies of Viruses by Raman Spectroscopy. This research was supported by the U.S. National Institutes of Health Grant GM50776.

* Author to whom correspondence should be addressed.

⊗ Abstract published in *Advance ACS Abstracts,* June 1, 1997.

S0006-2960(97)00342-5 CCC: $14.00

Table 1: Base Compositions and UV Extinction Coefficients of *fd* and *Pf1* Viruses and of ssDNA and dsDNA

	fd	Pf1	ssDNA[a]	dsDNA[b]
wt % DNA	12.1	6.3	100	100
base composition				
% A	25	20	25	28
% T	34	19	34	28
% G	21	30	21	22
% C	20	31	20	22
av nucleotide mol wt	323	325	323	323
extinction at λ_{max}	3.84[c]	2.12[c]	7200[d]	6300[d]
λ_{max} (nm)	270	272.5	260	260

[a] ssDNA extracted from *fd* virus. [b] dsDNA extracted from calf thymus nucleohistones. [c] Units of cm^2/mg (Day et al., 1988; Kostrikis et al., 1994). [d] Units of M^{-1} cm^{-1}.

In this work, we employ UVRR spectroscopy to probe specifically both the packaged ssDNA genome and the coat protein subunits of the filamentous virus *fd.* This has been accomplished by use of four different UV-laser excitation wavelengths, *viz.*, 257, 244, 238, and 229 nm. The 257-nm probe is virtually specific for the DNA nucleotides, while the 229-nm probe is essentially specific for tryptophan (W26) and tyrosine (Y21 and Y24) residues of the coat subunits. The UVRR spectra have been collected from both H_2O and D_2O solutions of *fd*, and all of the spectral intensities have been normalized by use of appropriate internal standards. Additionally, the UVRR spectra of *fd* have been compared quantitatively with UVRR data on viral constituents of known Raman scattering cross sections. The results obtained in this work are informative of the organization of the viral genome within the *fd* particle and of the environments of aromatic amino acid side chains of coat subunits. The present findings permit proposals to be made on the nature of interactions of ssDNA bases with one another and with coat protein subunits within the virion assembly. The accessibility of viral components to isotopic hydrogen exchange has also been revealed by deuteration studies. The present work represents the first application of the UVRR method for the development of a comprehensive scheme of Raman band assignments and quantitative analysis of the Raman scattering cross sections of a packaged viral DNA genome. The results provide a basis for future UVRR studies of *fd* and other filamentous virus assemblies.

EXPERIMENTAL METHODS

1. Materials. Growth media, standard reagents, amino acids, nucleosides, and deuterium oxide (99.8% D_2O) were obtained from Sigma Chemical (St. Louis, MO) and Fisher Scientific (St. Louis, MO). Double-stranded (ds) DNA of uniform size (160 base pairs), isolated from calf thymus, was a gift from Prof. Victor A. Bloomfield, University of Minnesota, St. Paul, MN. The *fd* virus was grown in MS media on *Escherichia coli* strain Hfr3300, using stocks obtained from Dr. Loren A. Day, Public Health Research Institute, New York, NY. Procedures for isolation, purification, and concentration of phage for Raman spectroscopic analysis have been described (Overman & Thomas, 1995). The concentrations of unpackaged *fd* DNA and calf thymus dsDNA were determined by UV absorption spectroscopy using the extinction coefficients in Table 1.

The purified bacteriophage was pelleted from 10 mM Tris buffer at pH 7.5. For UVRR spectroscopy, the *fd* sample was diluted to approximately 2 mg of virus/mL in the same buffer. Deuterated *fd* samples were prepared in an identical manner, except that D_2O replaced H_2O in the pelleting and dilution buffers. Sodium sulfate (Na_2SO_4) was added at precisely determined concentrations to virus solutions for use of its Raman band at 981 cm^{-1} as an absolute Raman intensity standard. Sodium ion concentration in the 100 mM range was found to have no significant effect upon the relative intensities of Raman bands of the viral DNA component, in accord with off-resonance Raman results (Thomas et al., 1983).

Protein-free single-stranded (ss) DNA was phenol-extracted from *fd* using standard protocols. Both *fd* ssDNA and calf thymus dsDNA were dissolved in the same buffer employed for the virus solutions.

2. Instrumentation and Sample Handling for UVRR Spectroscopy. UVRR spectra were excited at either 257, 244, 238, or 229 nm using a continuous-wave, frequency-doubled argon laser (Innova 300 FReD, Coherent Inc., Santa Clara, CA). Laser power at the sample was maintained at approximately 1 mW for excitations at 229, 238, and 244 nm and at approximately 5 mW for excitation at 257 nm. Raman scattering at 90° from a custom-designed, rotating (3000 rpm) quartz sample cell was analyzed using a single grating (2400 g/mm) spectrograph (Spex 750M, Instrument S. A., Edison, NJ) equipped with a prism predispersive element (McPherson Instruments, Acton, MA) and liquid nitrogen-cooled charge-coupled device detector (Instruments S. A.). The effective spectral resolution was 5 cm^{-1} or less. Further details of the design and performance characteristics of the UVRR instrument have been described (Russell et al., 1995).

Spectral data were collected at 20 °C and accumulated for up to 1 h. Raman frequencies were calibrated to ±1 cm^{-1} using a standard liquid mixture of carbon tetrachloride and acetonitrile. Corrections for the weak UVRR scattering of liquid water, gently sloping background, and spurious cosmic rays were carried out as previously described (Russell et al., 1995).

UVRR spectra of all biological samples (*fd*, ssDNA, dsDNA) showed no significant time dependence, indicating no appreciable photodecomposition from the data collection protocols (Russell et al., 1995). The integrity of the samples was confirmed following UVRR protocols by conventional UV absorption spectroscopy.

3. Data Analysis. (a) Raman Scattering Cross Sections. The scattering cross section (σ_n) of a Raman band of frequency ν_n may be obtained by comparison of its peak height (I_n) with the peak height (I_s) of an internal standard of known absolute Raman scattering cross section (σ_s) at frequency ν_s by use of eq 1:

$$\sigma_n = \sigma_s(I_n/I_s)(C_s/C_n)[(\nu_0 - \nu_s)/(\nu_0 - \nu_n)]^4 \qquad (1)$$

C_s and C_n are the molar concentrations of the internal standard and target molecule or residue(s), respectively, and ν_0 is the frequency of the exciting line, which is usually expressed in cm^{-1} units. Here, we employ as internal standard the prominent UVRR band of sodium sulfate at 981 cm^{-1}, which is assigned to the symmetrical stretching vibration of the SO_4^{2-} ion. Fodor et al. (1989) have determined the absolute Raman scattering cross section of the 981 cm^{-1} band of SO_4^{2-} as a function of excitation

wavelength in the ultraviolet region. From their results, we find $\sigma_s = 0.42$, 0.32, 0.24, and 0.16 millibarn at 229, 238, 244, and 257 nm, respectively.

In applying eq 1 to a Raman band of a particular nucleoside constituent of DNA, we replace C_n by C_b ($\equiv X_b C_n$, where X_b is the base mole fraction). C_b is estimated from the UV absorbance of DNA at 260 nm. For the packaged genomes of *fd* and *Pf1* virions, the molar concentration of a particular base is obtained from eq 2:

$$C_b = X_b C_n = X_b W f / M_{nuc} \quad (2)$$

where W is the weight concentration of the virion, which can be determined from the UV absorption spectrum and published extinction coefficients, f is the nominal weight fraction of DNA in the virion, and M_{nuc} is the average nucleotide molecular weight. Table 1 lists the appropriate information to apply eqs 1 and 2 to the DNA-containing samples investigated here.

In evaluating the Raman scattering cross section of a band assigned to a tryptophan or tyrosine residue of the *fd* virion, we make use of the known nucleotide:subunit ratio (2.3) and numbers of tryptophan (1) and tyrosine residues (2) per subunit (Day et al., 1988) in order to determine the molar concentrations of tryptophan (C_W) and tyrosine (C_Y); from which C_W:C_Y:C_n = 1:2:2.3.

(b) Raman Hypochromic Effects. It has long been recognized that the Raman scattering cross sections for certain ring vibrational modes of purine and pyrimidine residues in double-helical nucleic acids can be significantly smaller than those in constituent nucleosides, a phenomenon referred to as Raman *hypochromism* (Small & Peticolas, 1971; Thomas et al., 1972; Pézolet et al., 1975; Peticolas et al., 1987). Raman hypochromic effects have been attributed to stacking interactions of nucleic acid bases that depress electronic transition moments and hence the corresponding Raman intensities upon which they are dependent (through a fourth-power relationship) (Nishimura et al., 1978).

We define the hypochromicity of a DNA Raman band at frequency ν_n by the relation $1 - \gamma_n$, where the hypochromic ratio, γ_n, is the quotient of intensities in Raman spectra of the nucleic acid and constituent nucleoside(s). The term hypochromism properly refers to cases where $\gamma_n < 1$; conversely, hyperchromism implies $\gamma_n > 1$. In terms of the corresponding Raman scattering cross sections, γ_n is given by eq 3:

$$\gamma_n^{DNA} \equiv I_n^{DNA}/I_n^{nuc} = \sigma_n^{DNA}/\sigma_n^{nuc} \quad (3)$$

where σ_n^{DNA} and σ_n^{nuc} are Raman scattering cross sections for the band in DNA and in a solution of the free nucleoside, respectively.

By analogy with eq 3, we may similarly define γ_n^{prot} for a Raman band of a protein aromatic residue using eq 4:

$$\gamma_n^{prot} \equiv I_n^{prot}/I_n^{aa} = \sigma_n^{prot}/\sigma_n^{aa} \quad (4)$$

where σ_n^{prot} and σ_n^{aa} are Raman scattering cross sections for the residue in the protein and in a solution of the free amino acid.

(c) Experimental Uncertainties. The Raman scattering cross sections reported below are averages of multiple independent experiments exhibiting band intensity deviations of ±10% or less. Intensities were measured above a horizontal base line tangent to the wings of the band, following subtraction of the scattering background due to the quartz cell and sample buffer. The limits of error are due mainly to spectral noise and base line uncertainties. Sample self-absorption effects were avoided by focusing the UV laser beam at the inner front surface of the spinning sample cell to minimize the effective optical paths of incident and Raman-scattered photons. Other potential sources of error, such as polarization effects and sample photodecomposition, are virtually eliminated by the experimental design and data collection protocols, as previously described (Russell et al., 1995).

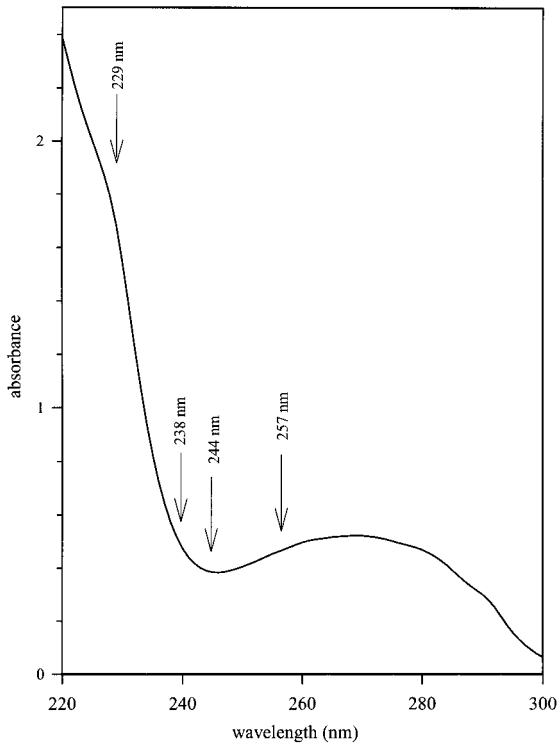

FIGURE 1: Ultraviolet absorption spectrum of *fd* virus in the wavelength interval 220−300 nm. Arrows indicate the laser wavelengths used to excite ultraviolet resonance Raman (UVRR) spectra displayed in subsequent figures. Virus concentration is approximately 0.60 mg/mL, and the optical path is 2 mm.

RESULTS

1. UVRR Spectra of fd Virus Excited at 257, 244, 238, and 229 nm. The UV absorption profile (220−300 nm) of *fd* and the laser wavelengths employed for excitation of UVRR spectra of the virus are indicated in Figure 1. The corresponding UVRR spectra (600−1800 cm^{-1}) of native *fd* in H_2O and D_2O solutions are shown in Figures 2 and 3, respectively. The data of Figures 2 and 3, which are of high signal-to-noise quality, illustrate the strong dependence of the UVRR spectrum of the virion upon excitation wavelength. This reflects the fact that the shorter UV wavelengths probe primarily the coat protein aromatics, tryptophan (W26) and tyrosine (Y21 and Y24), while the longer wavelengths probe primarily the base residues of the packaged ssDNA genome. Interestingly, despite the relatively low percentage (12%) of DNA contributing to the total virion mass, the Raman markers of the bases are intense and numerous in spectra excited at 257 nm (bottom traces of Figures 2 and 3).

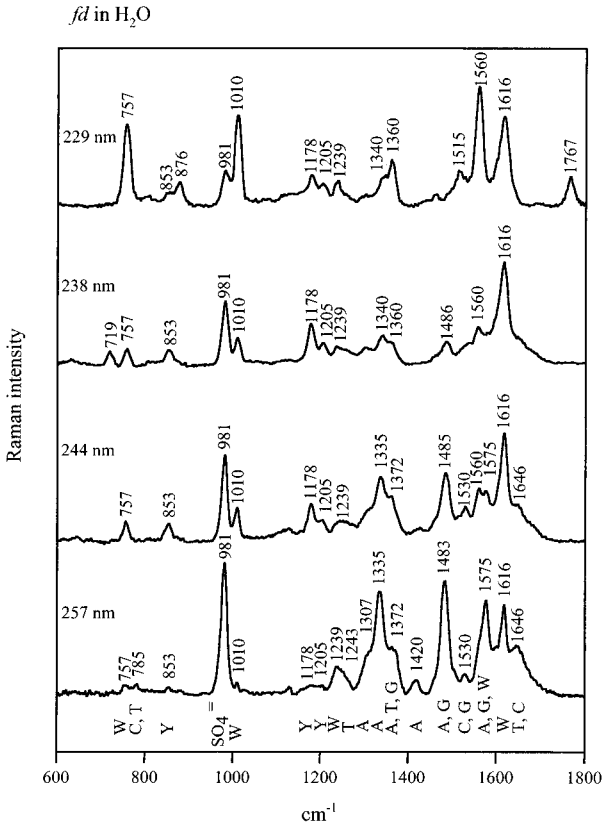

FIGURE 2: From top to bottom: UVRR spectra of H_2O solutions of *fd* virus, excited at 229, 238, 244, and 257 nm. Sample concentrations in terms of moles of DNA bases packaged are 0.18, 0.26, 0.49, and 0.54 mM, respectively (1 mM base concentration corresponds to 2.74 mg of virus/mL). The internal standard used for intensity calculations is the 981 cm^{-1} band of Na_2SO_4. The respective Na_2SO_4 concentrations are 166, 91, 100, and 91 mM. UVRR spectra were excited using laser powers of ~1 mW at 229, 238, and 244 nm and ~5 mW at 257 nm.

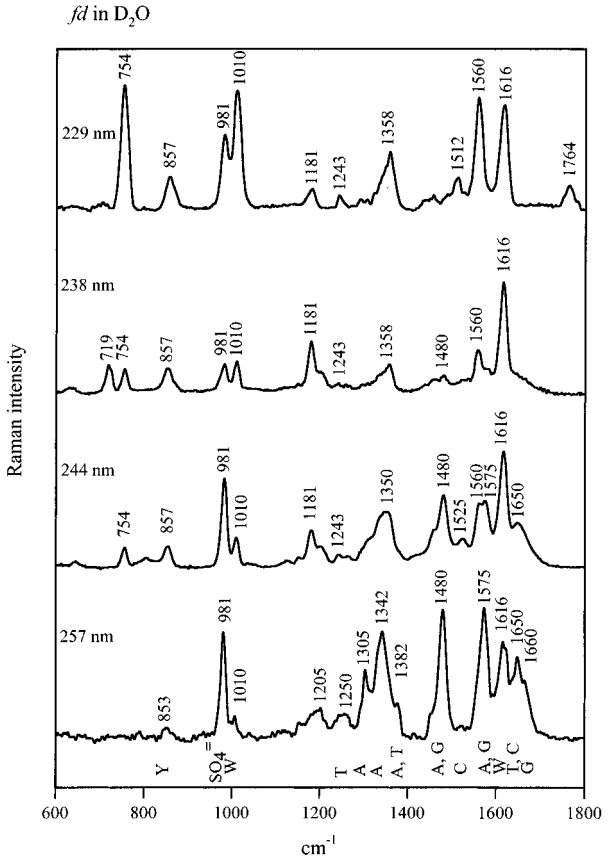

FIGURE 3: From top to bottom: UVRR spectra of D_2O solutions of *fd* virus, excited at 229, 238, 244, and 257 nm. Sample concentrations in terms of moles of DNA bases packaged are 0.16, 0.32, 0.43, and 0.57 mM, respectively. The respective Na_2SO_4 concentrations are 222, 87, 103, and 46 mM. Other conditions are as in Figure 2.

Phenylalanines (F11, F42, and F45), nonaromatic side chains and the polypeptide backbone of the coat protein subunits of *fd*, and also the phosphate and sugar residues of the ssDNA backbone are not represented significantly in any of the spectra of Figures 2 and 3. This is due to the fact that UV extinction coefficients for these moieties, and therefore their resonance Raman scattering cross sections, are too low in comparison to those of the DNA bases and of tryptophan and tyrosine side chains to be detected at the experimental conditions employed (Fodor et al., 1985, 1989; Asher et al., 1986; Takeuchi et al., 1996; Wen & Thomas, 1997).

2. Assignments and Characteristics of the UVRR Bands of fd. To facilitate the assignment of UVRR bands of *fd* (Figure 2) to specific bases of the packaged ssDNA and to aromatic amino acid side chains of the coat protein, we have carried out a comprehensive analysis of the UVRR spectra of aqueous solutions of deoxyadenosine (dA), deoxycytidine (dC), deoxyguanosine (dG), thymidine (dT), phenylalanine (F), tryptophan (W), and tyrosine (Y), using excitation wavelengths of 257, 244, 238, and 229 nm. The Raman scattering cross section of each prominent band in the UVRR spectrum of each viral constituent has been determined. The results, which are reported in detail elsewhere (Wen & Thomas, 1997), provide a reliable basis for assigning and interpreting the UVRR frequencies and intensities of the *fd* virion. The *fd* assignment scheme developed from the comprehensive UVRR analysis of nucleosides and aromatic amino acids is summarized in Table 2. These assignments are supported by three additional lines of experimental evidence: (i) UVRR band shifts resulting from deuteration of the virion (Figure 3), (ii) UVRR spectra obtained from protein-free ssDNA extracted from the *fd* virus (Figure 4), and (iii) off-resonance Raman spectra of the *fd* virus and its constituents published previously (Overman et al., 1994; Overman & Thomas, 1995) and reproduced in part in Figure 5.

Table 2 shows, as expected, that the 257-nm UVRR spectrum of *fd* is dominated by bands assignable to bases of the packaged genome. With one exception (*viz.*, the composite 1616 cm^{-1} band of tyrosines and tryptophan), the contributions from coat protein aromatics are feeble, resulting in very weak bands at 757, 853, 876, 1010, 1178, 1205, 1239, 1560, and 1616 cm^{-1}. Among the prominent DNA bands in the 257-nm excited UVRR spectrum, the strongest are associated with vibrational modes of adenine and guanine. This is consistent with earlier UVRR work on the nucleotides employing similar excitation wavelengths (Fodor et al., 1985; Tsuboi et al., 1987). The purine modes have been assigned to vibrations involving mainly in-plane stretching motions of the five- and six-membered heterocyclic moieties.

The DNA bases can be differentiated in the UVRR spectra of *fd* by their characteristic Raman band frequencies and intensities (cross sections). For example, adenine exhibits a very strong band at 1335 cm^{-1} when 257-nm excitation is employed (Figure 2, bottom trace). Because no other DNA

Table 2: Frequencies and Assignments of *fd* Virus in UVRR Spectra Excited at 257, 244, 238, and 229 nm[a]

257 nm	244 nm	238 nm	229 nm	residue[b]	vibrational mode[c]
		719		Y	CCH d
757 (−3)	757 (−3)	757 (−3)	757 (−3)	W	*W18*
785				T, C	ring s
853	853	853	853	Y	ring s
876			876 (−20)	W	*W17*, N1H d
1010	1010	1010	1010	W	*W16*, CC s
1178 (+3)	1178 (+3)	1178 (+3)	1178 (+3)	Y	*Y9a*
1205	1205	1205	1205	Y	*Y7a*
1239	1239	1239	1239	W	*W10*
1243				T	C2N3 s
1307 (−2)	1307 (−2)			A	C8H d, C8N7 s
		1340	1340	W	*W7* Fermi doublet
1335 (+7)	1335 (+7)			A	N7C5 s, C8N7 s
		1360 (−2)	1360 (−2)	W	*W7* Fermi doublet
1372	1372			A, T, G	C1N9 s, C6N6 s
1420	1420			A	C4C9 s, C8H d
	1485 (−4)	1486 (−5)		G	C8H d, N9C8 s
1483 (−3)				A	C2H d, N9C8 s
1507				A	N7C8 s
1530 (−5)	1530			C, G	N3C4 s
1560	1560	1560		W	*W3*, C2C3 s
1575 (−3)	1575 (−3)			G, A, W	C5C4, C4N3 s, *W2*
1616	1616	1616	1616	W, Y	*W1*, *Y8a*
1646 (+4)	1646 (+4)			T, C	C4═O, C5═C6 s
			1767	W	*W16* + *W18*

[a] For the excitation wavelength indicated at the top of columns 1−4, the UVRR frequencies of H_2O solutions are listed in cm^{-1} units. Values in parentheses indicate deuteration shifts observed for corresponding D_2O solutions. [b] A, C, G, and T indicate DNA bases; Y and W indicate tyrosine and tryptophan. [c] Vibrational assignments and nomenclature are based upon model compound studies (Lord & Thomas, 1967; Tsuboi et al., 1973, 1987; Fodor et al., 1985; Takeuchi & Harada, 1986; Takeuchi et al., 1988, 1989; Toyama et al., 1993; Overman & Thomas, 1995; Wen & Thomas, 1997). Abbreviations: s, stretching; d, deformation; b, bending.

base generates a 257-nm UVRR band near 1335 cm^{-1} (Wen & Thomas, 1997), this marker is diagnostic of adenine. Additionally, with 257-nm excitation, adenine generates a moderately intense band at 1482 cm^{-1} that is overlapped by a comparably intense band of guanine at 1485 cm^{-1}. However, when the excitation wavelength is shifted to 244 nm (Figure 2, second trace from bottom), the Raman cross section of the guanine 1485 cm^{-1} marker becomes 2-fold greater than that of the adenine 1482 cm^{-1} marker, such that the guanine marker dominates in the 244-nm spectrum. Moreover, these purine markers exhibit very different deuteration shifts. Thus, while the adenine marker at 1482 cm^{-1} is invariant to a change from H_2O to D_2O solution, the guanine marker at 1485 cm^{-1} (H_2O) is deuteration-sensitive, shifting to 1479 cm^{-1} in D_2O solution (Wen & Thomas, 1997). In comparison to the intense Raman markers of dA and dG residues in UVRR spectra excited at 257 nm, the pyrimidines exhibit marker bands of more modest intensity. For example, the dC and dT residues of packaged ssDNA are identified by their moderately intense bands near 1530 and 1650 cm^{-1}, respectively, in the *fd* spectrum of Figure 2 (bottom trace). The dC band at 1530 cm^{-1} has been assigned to a pyrimidine ring vibration, whereas the dT band near 1650 cm^{-1} is due largely to C4═O stretching. Interestingly, the cross section of the dC marker increases significantly in spectra excited at shorter wavelengths, while that of dT remains fairly constant. [Detailed UVRR spectra of the four DNA nucleosides excited at 257, 244, 238, and 229 nm and tabulations of the Raman scattering cross sections will be published elsewhere (Wen & Thomas, 1997). The data are also available as Supplementary Material, or upon request from the authors.]

The UVRR bands of the coat protein aromatics (W26, Y21, Y24) are represented most strongly in the spectrum obtained with 229-nm excitation (Figure 2, top trace). Because the UVRR scattering cross sections at 229 nm of the nucleosides are very much smaller than those of tryptophan or tyrosine (Wen & Thomas, 1997), no DNA bands of appreciable intensity appear at this excitation wavelength. The predominance of coat protein aromatic markers over those of the packaged ssDNA bases is promoted by two additional factors, *viz.*, the low mass of DNA in the virion and the effects of ssDNA secondary structure. The latter is further discussed below.

Many UVRR markers of W26, Y21, and Y24 in the spectrum of *fd* exhibit significant differences from corresponding spectra of the free amino acids in aqueous solution (Wen & Thomas, 1997). Notable among these are: (i) the indole ring mode *W3* occurring near 1550 cm^{-1} in free tryptophan, but at 1560 cm^{-1} in *fd*; (ii) the indole ring mode *W17*, occurring at 880 cm^{-1} in free tryptophan, but at 876 cm^{-1} in *fd*; (iii) the phenolic ring Fermi doublet {2*Y16a* + *Y1*} occurring at 850 and 830 cm^{-1} in free tyrosine, but as a singlet at 853 cm^{-1} in *fd*; (iv) the phenolic ring mode *Y7a* occurring at 1210 cm^{-1} in free tyrosine, but at 1205 cm^{-1} in *fd*. These and other differences between Raman markers of coat protein aromatics in the virion and of free amino acids are discussed below. [Detailed UVRR spectra of the aromatic amino acids excited at 257, 244, 238, and 229 nm and tabulations of the Raman scattering cross sections will be published elsewhere (Wen & Thomas, 1997). The data are also available as Supplementary Material, or upon request from the authors.]

DISCUSSION

1. Structural Interpretation of UVRR Markers of Packaged fd DNA. (a) Raman Hypochromism. The stacking of purine and pyrimidine bases in double-helical DNA sup-

presses the ultraviolet extinction coefficients of the bases and reduces the intensity of UV light absorption. For a fully base-stacked DNA structure, this intensity reduction (or UV hypochromism) is typically of the order of 40% of the absorbance at 260 nm. Because of the direct fourth-power relationship between intensities of UVRR scattering and UV absorption (Nishimura et al., 1978), the same factors which cause UV hypochromism are expected to affect even more significantly the UVRR spectral intensities. Accordingly, UVRR spectroscopy provides a sensitive probe of base-stacking interactions in DNA. Ultraviolet resonance Raman hypochromic effects have been reported previously for calf thymus DNA and related double-helical polydeoxynucleotides by Fodor and Spiro (1986).

To determine whether UVRR hypochromic effects are associated with the bases of the packaged *fd* genome, we compared the 257-nm excited UVRR spectrum of the virion with spectra of the following DNA samples. (i) Calf thymus double-stranded (ds) DNA: In this dsDNA, all bases are paired and stacked. (ii) Protein-free ssDNA extracted from *fd*: In this ssDNA, hairpin formation is expected to lead to appreciable base pairing and stacking, but a substantial proportion of the bases may be unpaired and/or unstacked. (iii) A mixture of mononucleosides corresponding to the base composition of *fd* DNA: In this nucleoside mixture, neither base pairing nor base stacking occurs to an appreciable extent. The mixture serves as a reference for estimating the magnitude of hypochromic effects in bases of ssDNA or dsDNA. The results are shown in Figure 4. Each sample of Figure 4 contains a known concentration of SO_4^{2-} to generate the sharp band at 981 cm^{-1} that is used as an internal intensity standard. Several interesting conclusions can be drawn from the results of Figure 4.

First, the prominent bands in the *fd* spectrum near 1243 (dT), 1307 (dA), 1335 (dA), 1372 (dA, dT, dG), 1420 (dA), 1483 (dA, dG), 1530 (dC, dG), and 1575 (dA, dG) cm^{-1} exhibit the same or nearly the same frequencies in isolated ssDNA, dsDNA, and the mixture of mononucleosides. Therefore, the frequencies of these base vibrations are not highly sensitive to secondary structure. Conversely, the *fd* band at 1646 cm^{-1} is significantly lower in frequency than the corresponding band (1650−1652 cm^{-1}) in all other samples. Thus, the carbonyl groups of dT, which are the major contributors to this band, evidently exist in an environment in the native *fd* virion that is different from the environments of thymine carbonyl groups of either dsDNA, ssDNA, or the aqueous nucleoside mixture.

Second, normalized UVRR intensities of the DNA bands (Raman cross sections, eq 1) are dramatically lower in *fd* than in the nucleoside mixture. This can be seen in Table 3. Surprisingly, the Raman cross sections of packaged *fd* DNA are even lower than those of calf thymus dsDNA. The extraordinarily large suppression of UVRR intensity (hypochromism, eq 2) for bases of the packaged *fd* genome is considered evidence of very strong interactions of the bases. Such interactions may involve the bases with one another or with coat protein subunits.

Third, the coat protein aromatics do not contribute appreciably to the *fd* spectrum, with the sole exception of a contribution from W26 at 1616 cm^{-1}. In computing the cross sections listed in Table 3, the very small contribution expected from W26 in the vicinity of 1560 cm^{-1} has been subtracted from the much greater purine contribution at 1575

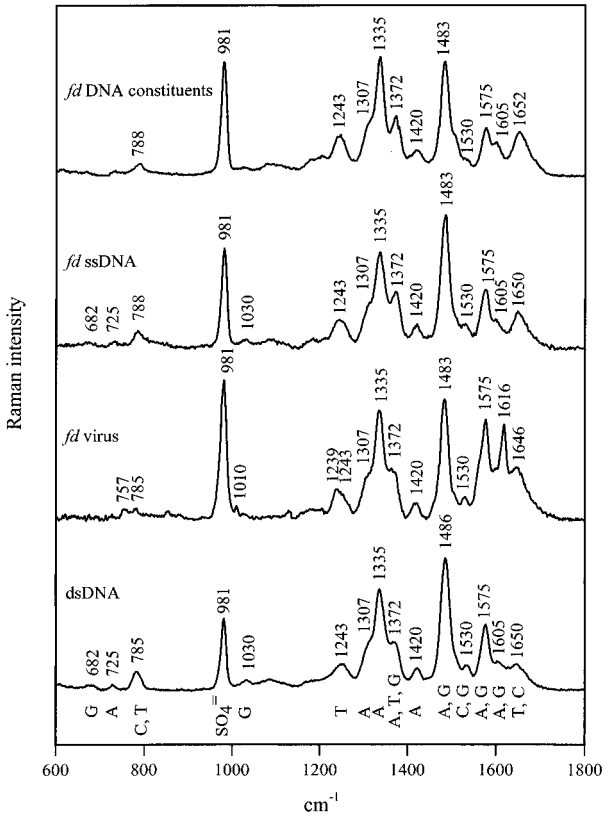

FIGURE 4: From top to bottom: UVRR spectra of a deoxynucleoside mixture (25% dA, 34% dT, 21% dG, 20% dC) corresponding to the base composition of *fd* DNA, unpackaged *fd* DNA, native *fd* virus, and dsDNA isolated from calf thymus (56% AT, 44% GC). Sample concentrations in terms of moles of DNA bases are 0.30, 0.74, 0.54, and 0.72 mM, respectively. The respective Na_2SO_4 concentrations are 200, 186, 91, and 100 mM. All UVRR spectra were excited at 257 nm.

cm^{-1}. This was accomplished by curve fitting the overlapped bands of the 1560−1650 cm^{-1} interval to Gauss−Lorentz components at 1560, 1575, 1600, 1616, and 1650 cm^{-1}, and subtracting the peak height at 1560 cm^{-1} from that at 1575 cm^{-1}. We have also included in Table 3 the Raman cross sections (eq 1) and hypochromic effects (eq 2) determined from the 257-nm excited UVRR spectrum of the *Pf1* filamentous virus (Z. Q. Wen, S. A. Overman, and G. J. Thomas, Jr., manuscript in preparation). Interestingly, in contrast to *fd*, the packaged ssDNA of *Pf1* does not exhibit large hypochromic effects. Further discussion of the remarkable differences between *fd* and *Pf1* with respect to UVRR hypochromicity of DNA markers is given below.

Table 3 shows that UVRR hypochromic effects for the DNA bases generally increase in the order: *Pf1* virion < ssDNA (unpackaged) < dsDNA < *fd* virion. The reference state (no hypochromism) is the mixture of mononucleosides. Surprisingly, the largest UVRR hypochromic effects—amounting to losses as large as 80% of the expected Raman band intensities—occur for the ssDNA packaged within the *fd* virion. Because all of the affected bands are associated with in-plane ring stretching modes of the bases (Lord & Thomas, 1967), the large UVRR hypochromic effects can be attributed to interactions which greatly perturb the π-electron densities in the heterocycles. By analogy with the case of double-helical DNA (Fodor & Spiro, 1986), we attribute the perturbations to either base stacking or interactions of the bases with coat protein subgroups. This

Table 3: UVRR Cross Sections (σ) and Hypochromic Ratios (γ) for Bands of the Purine and Pyrimidine Bases of *fd* Virus, *Pf1* Virus, ssDNA, and dsDNA[a]

	fd virus			*Pf1* virus			*fd* ssDNA			dsDNA		
band (cm^{-1})	σ^{DNA}	σ^{nuc}	γ	σ^{DNA}	σ^{nuc}	γ	σ^{DNA}	σ^{nuc}	γ	σ^{DNA}	σ^{nuc}	γ
1335	83	395	0.21	222	381	0.58	138	395	0.35	97	363	0.27
1483	60	244	0.25	198	230	0.86	124	244	0.51	84	220	0.38
1575	17	70	0.24	80	97	0.82	38	70	0.54	33	74	0.44
1640				200		1.70						
1646	32		0.29									
1650							39		0.36	26		0.23
1652		110			120			110			110	

[a] Cross sections for bands assigned to packaged or unpackaged DNA (σ^{DNA}) and to nucleosides (σ^{nuc}) are in millibarn units; hypochromic ratios are defined by eq 3. All data pertain to UVRR spectra excited at 257 nm. ssDNA and dsDNA are extracted from *fd* virus and calf thymus nucleohistones, respectively.

conclusion, which is reached solely from the UVRR results, is consistent with the similar conclusion drawn previously from UV absorption spectra of *fd* (Day, 1969). Fiber X-ray diffraction data also suggest that bases of the packaged *fd* genome are stacked (Banner et al., 1981), although diffraction from the DNA is very weak. Based upon the overall virion length and the number of bases in the circular ssDNA genome, Day and co-workers estimate an axial nucleotide separation of about 2.7 Å (Day, 1969; Day et al., 1988), similar to that of canonical *A* DNA (2.6 Å) but considerably less than that of canonical *B* DNA (3.4 Å) (Saenger, 1984). A small axial separation between bases of packaged *fd* DNA would favor appreciable stacking and is consistent with the large hypochromic effects observed in UVRR spectra.

Large UVRR hypochromic effects, whether due to extensive base stacking, to base-subunit interactions, or to a combination of both, might also explain the apparent absence of DNA Raman bands from previously reported UVRR spectra of *fd*. Grygon et al. (1988) noted that their attempts to excite UVRR spectra of *fd* at 266 and 240 nm were not successful in revealing any Raman markers of the packaged DNA.

(b) Anomalous Thymidine Marker at 1646 cm^{-1}. The UVRR band of *fd* at 1646 cm^{-1}, which is due to the packaged ssDNA molecule (Table 2) and which is assigned to a thymidine vibration involving the C4═O carbonyl group and the conjugated C5═C6 group (Tsuboi et al., 1997), occurs at a significantly lower frequency than its counterpart either in dsDNA (1650 cm^{-1}) or in aqueous solutions of thymidine mononucleosides (1655−1657 cm^{-1}) (Tsuboi et al., 1997; Wen & Thomas, 1997). This suggests an unusual hydrogen bonding state for the thymine C4═O groups in packaged *fd* DNA. One explanation for the lowering of the carbonyl stretching frequency to 1646 cm^{-1} in packaged *fd* DNA is that thymine C4═O groups within the virion are acceptors of *stronger* hydrogen bonds than occur either in conventional TA base pairs of dsDNA or in the solvent-exposed thymine base of aqueous thymidine.

2. Comparison with Other DNA Assemblies. Although the nature of DNA base interactions in *fd* cannot be deduced unambiguously from the UVRR data, it is instructive to compare the *fd* results with those obtained from other virions. Table 3 shows, for example, that the UVRR hypochromicities of packaged *fd* DNA (at 1335, 1483, and 1575 cm^{-1}, in particular) are much greater than those of packaged *Pf1* DNA, even though both filamentous virions comprise a single-stranded DNA loop encapsidated within a cylinder of small helical protein subunits. Therefore, the large UVRR hypochromic effects in *fd* cannot be attributed simply to enclosure of the DNA loop within a protein sheath. *The UVRR hypochromicities obviously reflect interactions of the bases that are specific to the* fd *architecture.*

Because the DNA bands of *Pf1* virus exhibit relatively little Raman hypochromism by comparison with *fd*, it is reasonable to conclude that the *Pf1* DNA bases are neither as extensively stacked nor as intimately associated with coat protein subunits in a manner that would diminish the Raman cross sections. This conclusion is in accord with interpretations of both UV absorption and CD spectra of *Pf1* (Kostrikis et al., 1994). It has also been noted that the length of the *Pf1* virion implies that the axial base separation could be as large as 6 Å, which certainly would disfavor base stacking interactions (Day et al., 1988). The present UVRR results provide direct evidence that the native *fd* and *Pf1* virions incorporate fundamentally different DNA structures. Strong base stacking interactions are consistent with the Raman signature of *fd*, but not with that of *Pf1*. Table 3 includes UVRR hypochromicities measured for a typical dsDNA having the *B* form secondary structure. Comparison of the data on *fd* DNA and *B* form dsDNA shows that UVRR hypochromicities of the former, particularly for bands of the purines at 1483 and 1575 cm^{-1}, are much greater than can be accounted for by base stacking arrangements analogous to those of a Watson-Crick secondary structure. Thus, we conclude further that putative stacking and/or hydrogen bonding interactions of the bases of the packaged *fd* genome differ dramatically from those of *B* form DNA.

In a detailed Raman study of the *Salmonella* bacteriophage *P22*, which packages a dsDNA genome, Aubrey et al. (1992) have demonstrated that condensation (packaging) of the dsDNA results in no appreciable Raman hypochromic effects beyond those observed for the uncondensed (unpackaged) genome. Therefore, the large UVRR hypochromic effects in *fd* cannot be attributed to condensation associated with DNA packaging. As noted above, the UVRR hypochromicities probably reflect interactions of the bases that are specific to the *fd* architecture.

3. Comparison with Other Structural Studies of fd. Glucksman et al. (1992) investigated the native *fd* (*M13)* virion, as well as chemically modified derivatives, by fiber X-ray diffraction and were not able to duplicate reflections of the type ascribed earlier by Banner et al. (1981) to the packaged ssDNA. These authors concluded, therefore, that the fiber X-ray diffraction data provide no direct information about the structure of the packaged DNA. Nevertheless, on the basis of their X-ray model for the coat protein,

Glucksman et al. (1992) proposed that DNA of the *B* form cannot be packaged within the hollow core of the virion. Our results provide direct evidence in support of such a proposal. Glucksman et al. (1992) proposed further that "the specific structural form of the packaged viral DNA is unimportant for viral structure and assembly". The present UVRR results, particularly the extraordinarily large UVRR hypochromic effects, suggest otherwise.

Two other lines of evidence support the notion of a preferred conformation for packaged *fd* DNA. First, the off-resonance Raman spectra of *fd* exhibit a definitive DNA marker near 665 cm^{-1} (Thomas et al., 1988; Aubrey & Thomas, 1991; Overman, 1996) that is diagnostic of C3′-*endo*/*anti* conformers of deoxyguanosine (Thomas & Wang, 1988) in the packaged ssDNA molecule. The intensity of this Raman marker indicates that the C3′-*endo*/*anti* conformation prevails for most, if not all, dG residues. Furthermore, no marker other than C3′-*endo*/*anti* dG (Thomas & Wang, 1988) is evident in the *fd* spectrum. Since dG is distributed throughout the genome, it is most likely that the C3′-*endo*/*anti* dG conformers are also widely distributed. Similar C3′-*endo*/*anti* conformers are expected for the other nucleosides. This is supported by the UVRR band near 1240 cm^{-1} (Figure 2), which is consistent with C3′-*endo*/*anti* thymidine conformers (Thomas & Wang, 1988). Second, UV linear dichroism (LD) studies of *fd* provide independent evidence of preferred base-plane orientations with respect to the virion axis (Clack & Gray, 1992). In fact, the UVLD studies of Clack and Gray (1992) and independent Raman linear intensity difference (RLID) studies of Takeuchi et al. (1996) are both consistent with base planes inclined at angles in the range 50−65°.

Solid-state ^{31}P-NMR spectra of oriented *fd* fibers have been interpreted as indicative of nonpreferential orientation of the phosphate groups in the packaged ssDNA (Cross et al., 1983). Unoriented phosphates on the NMR time scale are not inconsistent with ordering of the base residues or with conformational regularity in the sugar moieties as indicated by the Raman, UVRR, RLID, and UVLD measurements.

4. Structural Interpretation of UVRR Markers of fd Coat Protein. (a) Tryptophan-26. UVRR spectra excited at 229 and 238 nm provide structural information regarding the unique tryptophan residue (W26) of the coat protein subunit. Most informative are the bands near 1540−1560 cm^{-1} (normal mode *W3*), near 1340 and 1360 cm^{-1} (a Fermi doublet involving normal mode *W7* and an unspecified overtone or combination band *W7′*), and near 875−880 cm^{-1} (normal mode *W17*) (Harada et al., 1986; Miura et al., 1988, 1989). Table 4 compares the UVRR cross sections of these and other tryptophan bands of *fd* with their counterparts in UVRR spectra of the free amino acid. The tryptophan markers exhibit much larger UVRR cross sections in the virus, i.e., large *hyper*chromicities relative to the free amino acid (eq 4, above). We also compared the UVRR cross sections of residue W26 of *fd* with the corresponding cross sections for a solvent-exposed tryptophan side chain in a well-characterized protein structure, *viz.*, the extracellular domain of the tumor necrosis factor receptor (αTNFR) (Tuma et al., 1995). In this αTNFR structure, the UVRR fingerprint is characterized by cross sections for tryptophan markers that are generally less than half as large as those of W26 (Wen & Thomas, 1997). High UVRR cross sections for tryptophan have been correlated by Efremov et al. (1992) as diagnostic of a hydrophobic indole ring environment. We conclude, therefore, that residue W26 in subunits of the *fd* assembly exists in a highly hydrophobic environment. The same conclusion has been reached previously from off-resonance Raman spectra of *fd* (Aubrey & Thomas, 1991; Overman & Thomas, 1995). In addition, we note that the position of the *W3* marker in the UVRR spectrum (1560 cm^{-1}) is identical to that observed in the off-resonance Raman spectrum and confirms an unusually large value (120°) for the magnitude of the side-chain torsion angle $\chi^{2,1}$ (C2−C3−Cβ−Cα).

Table 4: UVRR Cross Sections (σ) and Hyperchromic Ratios (γ) for Bands of the *fd* Coat Protein Tryptophan and Tyrosine Residues[a]

band (cm^{-1})	$\sigma^{fd(coat)}$	σ^{W}	σ^{Y}	γ
757	2380	847	−	2.8
853	130	−	45	2.9
1010	2250	570	−	3.9
1178	310	−	168	1.8
1552/1560[b]	2510	763	−	3.3

[a] Cross sections for bands assigned to *fd* coat protein residues W26 or Y21+Y24 ($\sigma^{fd(coat)}$) and to free amino acids (σ^{W}, σ^{Y}) are in millibarn units; hyperchromic ratios are defined by eq 4. All data pertain to UVRR spectra excited at 229 nm. [b] This indole ring marker (normal mode *W3*) occurs at 1560 cm^{-1} in *fd* coat protein and at 1552 cm^{-1} in the free amino acid (Miura et al., 1989; Aubrey & Thomas, 1991).

The tryptophan Raman markers are fully consistent with other spectroscopic results. For example, solid-state NMR spectra reveal that W26 in *fd* is immobile on the millisecond time scale (Cross et al., 1983). Fluorescence quenching data show a very high quantum yield for W26, a characteristic typical of tryptophan packed in a hydrophobic environment (Day et al., 1988). Interestingly, the observed UVRR hyperchromism (Table 4) is also quantitatively consistent with the UV absorption hyperchromism (≈30%) previously reported by Day (1969), i.e., $2.9 \approx (1.3)^4$.

The UVRR spectra of *fd* in D_2O solution, obtained by 229 and 238 nm excitations (Figure 3), confirm all of the conclusions reached from H_2O solution spectra and show in addition that the indole N1H group is not protected against deuterium exchange. The latter is evidenced by the 19 cm^{-1} shift to lower frequency (876 → 857 cm^{-1}) of the band assigned to normal mode *W17*. Thus, despite the hydrophobic environment of the indole moiety, its N1 proton is readily exchanged by D_2O solvent.

(b) Tyrosine-21 and Tyrosine-24. Table 4 shows that UVRR cross sections for marker bands of tyrosine, like those of tryptophan, are several times greater than their counterparts in the free amino acid. By analogy with tryptophan, these results are interpreted as indicative of hydrophobic ring environments for Y21 and Y24. This conclusion is consistent with the findings from off-resonance Raman spectra of *fd* (Overman et al., 1994; Overman & Thomas, 1995). Also in accord with the off-resonance Raman signature of *fd* is the absence of a canonical Fermi doublet (850/830 cm^{-1} doublet; Siamwiza et al., 1975) for tyrosines Y21 and Y24. The UVRR spectra of *fd*, particularly those excited at 238 and 244 nm (Figures 2 and 3), exhibit the anomalous tyrosine singlet (853 cm^{-1}) reported previously (Overman et al., 1994).

UVRR spectra of *fd* in D_2O show a clearcut deuteration shift of the 1178 cm^{-1} tyrosine marker to 1181 cm^{-1} (Takeuchi et al., 1989), indicating that both phenoxyl protons

are readily exchanged by solvent. Solvent accessibility of the exocyclic phenoxyls, notwithstanding the proposed hydrophobic environments for the aromatic rings, is analogous to the situation noted above for residue W26.

5. Hydrogen Isotope Exchange of Packaged ssDNA. It is of interest to determine whether the base amino and imino protons of packaged ssDNA can be exchanged by simply exposing the virion to D_2O solvent. [The peptide NH sites of viral coat subunits, unlike the NH and OH sites of tryptophan and tyrosine side chains, cannot all be exchanged at native conditions (Overman, 1996).] In principle, the question of DNA base exchanges may be addressed using a recently developed off-resonance Raman dynamic probe (Li et al., 1993; Tuma & Thomas, 1996). In practice, however, interference from the much stronger Raman bands of coat protein subunits precludes conclusive results from the off-resonance Raman spectrum (Overman, 1996). The data of Figure 3 show that this question can be addressed by UVRR and that the exchangeable base sites of packaged *fd* DNA are readily deuterated upon exposure of the native virion to D_2O solvent. Although no time resolution of the base exchanges has been attempted, the bases are completely exchanged in the minimum time required to prepare the sample in D_2O and collect the data (several hours). Conversely, some of the peptide NH groups of the coat protein are known to resist NH → ND exchange for months at native conditions (Williams et al., 1984; Overman, 1996).

Representative UVRR frequency shifts diagnostic of base amino/imino exchanges are the following: 1335 → 1342 cm^{-1} (dA), 1483 → 1480 cm^{-1} (dG), 1527 → 1505 cm^{-1} (dC), and 1646 → 1650 cm^{-1} (dT) (Wen & Thomas, 1997). Of these, all but the dC marker are clearly evident in Figures 2 and 3.

SUMMARY AND CONCLUSIONS

Ultraviolet resonance Raman spectra of the filamentous bacterial virus *fd* have been obtained at four excitation wavelengths, 257, 244, 238, and 229 nm. The spectrum excited at 257 nm, which is dominated by Raman markers of the packaged single-stranded DNA genome, provides a unique analytical fingerprint of the DNA bases and is informative of their structural context within the virion. The UVRR spectra excited at shorter wavelengths are dominated by tryptophan-26 (229 nm), or tyrosine-21 and tyrosine-24 (238 nm), or both the tyrosines and the DNA bases (244 nm). All of the UVRR band intensities have been interpreted on a quantitative basis by use of an internal intensity standard (SO_4^{2-}, 981 cm^{-1} band) of known Raman cross section. The present results provide a valuable complement to previously reported off-resonance Raman probes of *Ff* viruses (Thomas et al., 1983; 1988; Aubrey & Thomas, 1991; Overman & Thomas, 1995). Collectively, the UVRR spectra furnish new insights into the environments and interactions of the ssDNA bases and also confirm structural conclusions reached previously regarding both the DNA bases and coat protein aromatics.

The novel conclusions reached from this work center on the structure of the packaged viral genome. First and foremost, the UVRR markers of the *fd* genome are distinguished from those of all other DNA molecules examined, whether single- or double-stranded, by spectacular hypochromic effects. For key Raman markers of packaged *fd* DNA, as much as 80% of the expected UV resonance Raman band intensity is suppressed in the virion assembly. This phenomenon is believed due to specific and strong short-range interactions involving the DNA bases. We attribute the hypochromicities principally to base−base interactions; however, interactions of the bases with coat protein subgroups may also be a contributing factor. At present, no model systems are available to assess quantitatively the effects of DNA base-aromatic amino acid interactions on UVRR cross sections. Because Raman markers of all bases (A, T, G, C) are affected, the UVRR hypochromism is presumed to reflect base interactions distributed throughout the viral filament.

A second remarkable feature of the Raman signature of the packaged *fd* genome is a thymidine carbonyl (C4═O group) marker band displaced to unusually low frequency when compared with the solvated thymidine nucleoside and thymidines in other DNA structures. We have attributed this shift to unusually strong hydrogen bonding interactions of thymine C4═O acceptors in the virion. The putative hydrogen bonding donor is not known. However, because the thymine C4═O marker band of packaged *fd* DNA is significantly lower in frequency than its counterpart in dsDNA, it is reasonable to assume that the low frequency is not due simply to hydrogen bonding with adenines. The thymine marker of packaged *fd* DNA may reflect interactions with the protein coat.

A third noteworthy characteristic of the packaged *fd* genome is the occurrence of its conformation-sensitive dG Raman marker at 668 ± 2 cm^{-1} in the off-resonance Raman spectrum (Thomas et al., 1988), a frequency that is diagnostic of the nucleoside C3′-*endo/anti* conformation (Benevides & Thomas, 1983; Thomas & Wang, 1988). Such dG conformers are not normally stable in aqueous DNA, but do occur in the low-humidity structure (*A* form) of dsDNA fibers. Unfortunately, the UVRR cross section of the 668 cm^{-1} marker is very small in comparison to UVRR cross sections of the 1000−1800 cm^{-1} region (Wen & Thomas, 1997), thus precluding its detection in the spectra of Figures 2 and 3. (Hypochromism may also contribute to the difficulty in detecting a UVRR band near 668 cm^{-1} in *fd*.) Interestingly, the *fd* DNA molecule, when extracted from the virion, exhibits its off-resonance dG marker at 682 cm^{-1}, as expected for DNA containing C2′-*endo/anti* dG conformers (Thomas et al., 1988; Thomas & Wang, 1988). This is normally the lowest energy structure of DNA in solution. The 682 cm^{-1} marker is also evident in the UVRR spectra of dsDNA and extracted ssDNA (Figure 4).

We have confirmed the important differences between packaged and unpackaged *fd* DNA in the 600−750 cm^{-1} interval of the off-resonance Raman spectrum (514.5 nm excitation), as shown in Figure 5. Also included in Figure 5 is the Raman profile of dsDNA from *P22* virus, as well as data collected from corresponding D_2O solutions. The latter are important to illustrate the clearcut deuteration shift of the nearby dT marker in each DNA sample (Thomas & Benevides, 1985; Tsuboi et al., 1997), thus distinguishing it from the dG marker that is deuteration-insensitive (Benevides & Thomas, 1983; Miura & Thomas, 1995). Accordingly, in the *B* form duplex as well as in the protein-free ssDNA molecule extracted from *fd*, the C2′-*endo/anti* dG conformation prevails. Conversely, in the packaged ssDNA molecule, the C3′-*endo/anti* dG conformation is stabilized. Therefore,

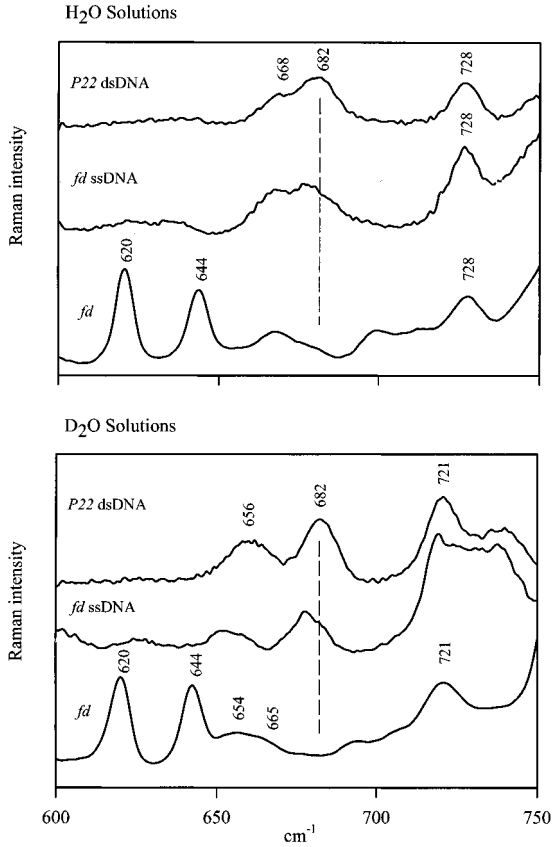

FIGURE 5: Off-resonance Raman spectra (514.5-nm excitation) of representative DNA structures and of the *fd* virus in H_2O (top panel) and D_2O solutions (bottom panel). The dsDNA (top trace in both panels) was isolated from *P22* virus; the ssDNA (middle traces) was isolated from *fd* virus; the native *fd* virus (bottom traces) was identical to samples yielding data of Figures 2 and 3. The interval shown here (600−750 cm^{-1}) contains the well-characterized Raman marker of the C2′-*endo/anti* conformation of dG (682 cm^{-1}), a band which is not sensitive to deuteration (Benevides & Thomas, 1983; Thomas & Wang, 1988). The marker is dominant in the spectrum of dsDNA and contributes to the spectrum of ssDNA; however, it is clearly absent from the spectrum of the packaged genome. Other bands of this interval are discussed in the text and have been described in more detail in previously published work (Thomas et al., 1983, 1988; Aubrey & Thomas, 1991; Overman & Thomas, 1995).

the organization of ssDNA within the *fd* virion and the interactions of its nucleotide residues impose an unusual furanose pucker for dG residues. Because dG is distributed throughout the genome, the unusual C3′-*endo/anti* conformation is also widely distributed. We propose that C3′-*endo/anti* conformers also prevail for other nucleosides of packaged *fd* DNA. This proposal is consistent with the observed UVRR markers of dA, dC, and dT.

Finally, with respect to the amino and imino protons of the DNA bases, we find no protection against hydrogen-isotope exchange conferred by the viral protein coat. This conclusion is limited by the low time-resolution (several hours) of the present measurements. Nevertheless, we can conclude that solvent molecules penetrate the protein coat of *fd*, and that exchange of guanine exocyclic groups in the packaged ssDNA is not precluded by highly structured networks of hydrogen bonds (Miura & Thomas, 1995).

While the UVRR intensities of packaged *fd* DNA are dramatically suppressed (hypochromism), we find that those of the coat protein aromatics, Y21, Y24, and W26, are correspondingly enhanced (hyperchromism) (Table 4). On the basis of model protein studies (Efremov et al., 1992), hyperchromism of UVRR bands of tryptophan is indicative of a hydrophobic indole ring environment. Hydrophobic environments for the indole moiety of W26, as well as for the *p*-phenyl moieties of Y21 and Y24, are consistent with off-resonance Raman markers of these residues (Aubrey & Thomas, 1991; Overman et al., 1994; Overman & Thomas, 1995) and with models proposed previously for packing of coat subunits in the *fd* assembly (Marvin et al., 1994; Overman et al., 1996). The present conclusions are also consistent with the findings reported previously for phenylalanyl side chains (F11, F42, and F45) of the *fd* subunit (Grygon et al., 1988; Overman et al., 1994). Nevertheless, despite the hydrophobic sequestration of pVIII aromatics in *fd*, we find that their polar substituents are not protected from hydrogen-isotope exchange. Thus, the indole N1H and phenoxyl OH protons of coat subunits are readily exchanged by deuterium in D_2O solutions of *fd*. This likely places the exocyclic protons either at the interface with the packaged ssDNA molecule or at the solvent-exposed surface of the virion.

In connection with the present study of *fd* (a class I filamentous virion), we have also obtained the UVRR fingerprint of the class II virion *Pf1*. The distinction between class I and class II architecture, which is based upon the respective fiber X-ray diffraction patterns, relates to the proposed symmetry of packing of the α-helical coat protein subunits (Makowski, 1984; Day et al., 1988). Surprisingly, although the *Pf1* virion contains only about 6% by weight DNA (roughly half that of *fd*), the UVRR markers of its packaged ssDNA molecule are far more intense than those of *fd* (Table 3). The coat subunit of *Pf1* is distinguished from that of *fd* by the absence of tryptophan, thus providing an opportunity for greater spectral access of UVRR markers of DNA and tyrosine using 238 and 229 nm excitations, respectively. A detailed analysis of the UVRR spectrum of *Pf1* will be reported in a forthcoming paper (Z. Q. Wen, S. A. Overman, and G. J. Thomas, Jr., manuscript in preparation). It will also be of interest to compare the present results on *fd* with UVRR spectra of other filamentous viruses, particularly the *Pf3* virion, a class II particle which contains a single tryptophan residue per coat subunit. Biophysical investigations of DNA structures and interactions in filamentous viruses have traditionally been plagued by the relatively low DNA mass composition in these particles. The present study demonstrates the value of the ultraviolet resonance Raman method as a probe of DNA organization within the filamentous virions.

ACKNOWLEDGMENT

We thank our colleagues, Drs. James M. Benevides and Laurent Laporte, for constructive comments on the manuscript.

REFERENCES

Arnold, G. E., Day, L. A., & Dunker, A. K. (1992) *Biochemistry 31*, 7948−7956.

Asher, S. A., Ludwig, M., & Johnson, C. R. (1986) *J. Am. Chem. Soc. 108*, 3186−3197.

Asher, S. A., Bormett, R. W., Chen, X. G., Lemmon, D. H., Cho, N., Peterson, P., Arrigoni, M., Spinelli, L., & Cannon, J. (1993) *Appl. Spectrosc. 47*, 628−633.

Aubrey, K. L., & Thomas, G. J., Jr. (1991) *Biophys. J. 60*, 1337−1349.
Aubrey, K. L., Casjens, S. R., & Thomas, G. J., Jr. (1992) *Biochemistry 31*, 11835−11842.
Austin, J. C., Jordan, T., & Spiro, T. G. (1993) in *Advances in Spectroscopy* (Clark, R. J. H., & Hester, R. E., Eds.) Vol. 20A, pp 55−127, Wiley & Sons, London.
Banner, D. W., Nave, C., & Marvin, D. A. (1981) *Nature 289*, 814−816.
Benevides, J. M., & Thomas, G. J., Jr. (1983) *Nucleic Acids Res. 11*, 5747−5761.
Clack, B. A., & Gray, D. M. (1992) *Biopolymers 32*, 795−810.
Cross, T. A., Tsang, P., & Opella, S. J. (1983) *Biochemistry 22*, 721−725.
Day, L. A. (1969) *J. Mol. Biol. 39*, 265−277.
Day, L. A., Marzec, C. J., Reisberg, S. A., & Casadevall, A. (1988) *Annu. Rev. Biophys. Biophys. Chem. 17*, 509−539.
Efremov, R. G., Feofanov, A. V., & Nabiev, I. R. (1992) *J. Raman Spectrosc. 23*, 69−73.
Fodor, S. P. A., & Spiro, T. G. (1986) *J. Am. Chem. Soc. 108*, 3198−3205.
Fodor, S. P. A., Rava, R. P., Hays, T. R., & Spiro, T. G. (1985) *J. Am. Chem. Soc. 107*, 1520−1529.
Fodor, S. P. A., Copeland, R. A., Grygon, C. A., & Spiro, T. G. (1989) *J. Am. Chem. Soc. 111*, 5509−5518.
Glucksman, M. J., Bhattacharjee, S., & Makowski, L. (1992) *J. Mol. Biol. 226*, 455−470.
Grygon, C. A., Perno, J. R., Fodor, S. P. A., & Spiro, T. G. (1988) *BioTechniques 6*, 50−55.
Harada, I., Miura, T., & Takeuchi, H. (1986) *Spectrochim. Acta 42A*, 307−312.
Kostrikis, L. G., Liu, D. J., & Day, L. A. (1994) *Biochemistry 33*, 1694−1703.
Li, T., Johnson, J. E., & Thomas, G. J., Jr. (1993) *Biophys. J. 65*, 1963−1972.
Lord, R. C., & Thomas, G. J., Jr. (1967) *Spectrochim. Acta 23A*, 2551−2591.
Makowski, L. (1984) in *Biological Macromolecules and Assemblies* (McPherson, A., Ed.) Vol. 1, pp 203−253, Wiley, New York.
Marvin, D. A., Hale, R. D., Nave, C., & Citterich, M. H. (1994) *J. Mol. Biol. 235*, 260−286.
McDonnell, P. A., Shon, K., Kim, Y., & Opella, S. J. (1993) *J. Mol. Biol. 233*, 447−463.
Miura, T., & Thomas, G. J., Jr. (1995) *in Subcellular Biochemistry: Structure, Function and Engineering* (Biswas, B. B., & Roy, S., Eds.) Plenum, New York.
Miura, T., Takeuchi, H., & Harada, I. (1988) *Biochemistry 27*, 88−94.
Miura, T., Takeuchi, H., & Harada, I. (1989) *J. Raman Spectrosc. 20*, 667−671.
Nishimura, Y., Hirakawa, A. Y., & Tsuboi, M. (1978) in *Advances in Infrared and Raman Spectroscopy* (Clark, R. J. H., & Hester, R. E., Eds.) Vol. 5, pp 217−275, Heyden, London.
Overman, S. A. (1996) Ph.D. Thesis, School of Biological Sciences, University of Missouri, Kansas City, MO.
Overman, S. A., & Thomas, G. J., Jr. (1995) *Biochemistry 34*, 5440−5451.
Overman, S. A., Aubrey, K. L., Vispo, N. S., Cesareni, G., & Thomas, G. J., Jr. (1994) *Biochemistry 33*, 1037−1042.
Overman, S. A., Tsuboi, M., & Thomas, G. J., Jr. (1996) *J. Mol. Biol. 259*, 331−336.
Peticolas, W. L., Kubasek, K. L., Thomas, G. A., & Tsuboi, M. (1987) in *Biological Applications of Raman Spectroscopy* (Spiro, T. G., Ed.) Vol. 1, pp 81−133, Wiley-Interscience, New York.
Pézolet, M., Yu, T. J., & Peticolas, W. L. (1975) *J. Raman Spectrosc. 3*, 55−64.
Russell, M. P., Vohník, S., & Thomas, G. J., Jr. (1995) *Biophys. J. 68*, 1607−1612.
Saenger, W. (1984) *Principles of Nucleic Acid Structure*, Springer-Verlag, New York.
Siamwiza, M. N., Lord, R. C., Chen, M. C., Takamatsu, T., Harada, I., Matsuura, H., & Shimanouchi, T. (1975) *Biochemistry 14*, 4870−4876.
Small, E. W., & Peticolas, W. L. (1971) *Biopolymers 10*, 69−88.
Symmons, M. F., Welsh, L. C., Nave, C., Marvin, D. A., & Perham, R. N. (1995) *J. Mol. Biol. 245*, 86−91.
Takeuchi, H., & Harada, I. (1986) *Spectrochim. Acta 42A*, 1069−1078.
Takeuchi, H., Watanabe, N., & Harada, I. (1988) *Spectrochim. Acta 44A*, 749−761.
Takeuchi, H., Watanabe, N., Satoh, Y., & Harada, I. (1989) *J. Raman Spectrosc. 20*, 233−237.
Takeuchi, H., Matsuno, M., Overman, S. A., & Thomas, G. J., Jr. (1996) *J. Am. Chem. Soc. 118*, 3498−3507.
Thomas, G. J., Jr., & Benevides, J. M. (1985) *Biopolymers 24*, 1101−1105.
Thomas, G. J., Jr., & Wang, A. H.-J. (1988) in *Nucleic Acids and Molecular Biology* (Eckstein, F., & Lilly, D. M. J., Eds.) Vol. 2, pp 1−30, Springer-Verlag, Berlin.
Thomas, G. J., Jr., & Tsuboi, M. (1993) *Adv. Biophys. Chem. 3*, 1−70.
Thomas, G. J., Jr., Medeiros, G. C., & Hartman, K. A. (1972) *Biochim. Biophys. Acta 277*, 71−79.
Thomas, G. J., Jr., Prescott, B., & Day, L. A. (1983) *J. Mol. Biol. 615*, 321−356.
Thomas, G. J., Jr., Prescott, B., Opella, S. J., & Day, L. A. (1988) *Biochemistry 27*, 4350−4357.
Toyama, A., Takino, Y., Takeuchi, H., & Harada, I. (1993) *J. Am. Chem. Soc. 115*, 11092−11098.
Tsuboi, M., Takahashi, S., & Harada, I. (1973) in *Physical Chemical Properties of Nucleic Acids* (Duchesne, J., Ed.) Vol. 2, pp 91−145, Academic Press, London.
Tsuboi, M., Nishimura, Y., Hirakawa, A. Y., & Peticolas, W. L. (1987) in *Biological Applications of Raman Spectroscopy* (Spiro, T. G., Ed.) Vol. 2, pp 109−179, Wiley-Interscience, New York.
Tsuboi, M., Overman, S. A., & Thomas, G. J., Jr. (1996) *Biochemistry 35*, 10403−10410.
Tsuboi, M., Komatsu, M., Hoshi, J., Kawashima, E., Sekine, T., Ishido, Y., Russell, M. P., Benevides, J. M., & Thomas, G. J., Jr. (1997) *J. Am. Chem. Soc. 119*, 2025−2032.
Tuma, R., & Thomas, G. J., Jr. (1996) *Biophys. J. 71*, 3454−3466.
Tuma, R., Russell, M. P., Rosendahl, M., & Thomas, G. J., Jr. (1995) *Biochemistry 34*, 15150−15156.
Tuma, R., Bamford, J. H. K., Bamford, D. H., Russell, M. P., & Thomas, G. J., Jr. (1996) *J. Mol. Biol. 257*, 87−101.
Wen, Z. Q., & Thomas, G. J., Jr. (1997) *Biopolymers* (submitted for publication).
Williams, R. W., Dunker, A. K., & Peticolas, W. L. (1984) *Biochim. Biophys. Acta 791*, 131−144.

BI970342Q